

A New Linear Matrix Method for Calculating Slot Less Permanent Magnets Motors

Andre YOUMSSI*

**Electric Energy Laboratory (LEE) - Montreal – Canada
– Ecole Polytechnique de Montreal, Succursale Centre Ville, C.P: 6079
– Montreal – Quebec – Canada –H3C 3A7
Corresponding author: Email: ande.youmssi@yahoo.com*

ABSTRACT.

This paper presents a systematic semi-analytical method for calculating the magnetic flux density in different linear media separated by concentric cylindrical surfaces. The proposed method consists in setting the expressions of the magnetic potentials with, or without the presence of ferromagnetic materials, depending on whether the sources are permanent magnets or electric currents that could here be modelled through magnetic charge densities or magnetic current densities, carried by any concentric cylindrical surface. The coefficients in the expressions of the magnetic potentials are obtained owing to boundary conditions that are written on the separation surface between two media. The originality and interest of this contribution lie in the fact that the calculation of the coefficients generates matrices which simplify the study and then make the here by proposed method systematic, and thus enabling the handling of models with a great number of magnetic regions, then allowing semi-analytical studies of the types of problems that usually have their solutions only possible through a numerical code. In this paper, the proposed method is validated through two case studies: a classical predictable example and a difficult case that concerns a permanent magnets motor with four magnetic media considered. The first application as well as the second one, which is also an analysis of a surface sector-shaped permanent magnets synchronous motor, show the same results when calculating the magnetic scalar potentials, and the magnetic flux density, using the present proposed systematic linear method, the classical method of the separations expressions of variables, the method of magnetic images and a numerical method based on finite differences.

Key Words— Analytical technique, electrical motor modeling and design, Permanent- Magnets Motors

LIST OF PRINCIPAL SYMBOLS:

a:	an arbitrary boundary.
A:	a matrix.
A_z :	component of the vector potential with respect to z-axis.
A_{zi} :	component of the vector potential with respect to z-axis for $r < R$
A_{ze} :	component of the vector potential with respect to z-axis for $r > R$
A_{zk} :	component of the vector potential with respect to z-axis in medium k.
B:	magnitude of the magnetic flux density vector in the permanent magnet synchronous Machine
$B_r(r, \theta)$:	radial component of the magnetic flux density vector.
H:	magnitude of the magnetic field vector in the permanent magnet synchronous Machine
a_k :	coefficient of harmonics in series expansions.
b_k :	coefficient of harmonics in series expansions.
$h_1, h_2, h_3, h_4, h_7, h_8, h_9, h_{10}$:	coefficients used in the method of magnetic images.
H_c :	coercive field.
I:	a matrix.
k:	surface current density, also index (explained in the text).
K_o :	magnitude of the fundamental rank of k.
M:	a matrix.
M_{rad} :	magnitude of the magnet magnetization vector.
M_1 :	a matrix.
M_2 :	a matrix.
n:	an index.
p:	number of pole-pair.
Q:	a matrix.
r:	position of the studied point in polar coordinates.
S:	a matrix.
R_1 :	radius of the boundary of medium 1.
R_2 :	radius of the boundary of medium 2.
R' :	interior radius of the permanent magnets
R:	exterior radius of the permanent magnets
R_k :	radius of the boundary of medium k.
\vec{M}_{rad} :	Magnet magnetization vector.
\vec{B} :	Magnetic flux density vector in the permanent magnet Synchronous machine
\vec{H} :	Magnetic field vector in the permanent magnet synchronous machine.
T_1 :	a matrix.

T_2 :	a matrix.
U :	a matrix.
V :	a matrix.
V^* :	the magnetic scalar potential.
X :	a matrix.
z :	any complex number.
OB :	position of the magnetic image σ'^*
α :	a matrix.
α_k :	coefficient of harmonics in series expansions.
β_k :	coefficient of harmonics in series expansions.
γ :	a matrix.
μ :	Magnetic permeability of a medium.
μ_k :	magnetic permeability of the media of index k.
μ_o :	magnetic permeability of free space.
μ_r :	relative magnetic permeability of the magnet
v :	Rank of harmonics in Fourier's series.
θ :	Angle of the studied point in polar co-ordinates.
$d\theta$:	differential angle of the studied point in polar co-ordinates
θ_o :	origin angle.
θ_{ra} :	width of a permanent magnet
ρ^* :	volume charge density.
σ^* :	magnetic surface charge density.
σ'^* :	magnetic image of σ^* which appears on the surface OB.
σ''^* :	magnetic image of σ^* which appears on the surface R.
σ_o^* :	amplitude of the fundamental rank of σ^* .
Ψ_k :	complex magnetic potential.

I. INTRODUCTION.

In designing electrical rotating cylindrical machines or equivalent similar systems, the calculation of the potentials and the flux densities in relation to the sources, is usually carried out in two dimensions, with a limited number of media and usually considering an infinite permeability, the determination of the magnetic potentials and the flux densities then become feasible with difficulties depending on the studied cases. The proposed method particularly suits to the pre dimensioning of linear cylindrical rotating motors such as surface permanent magnets synchronous motors. It is semi analytical and easier to manipulate than what already exists in literature [1-16].

Moreover when the number of involved magnetic media is reasonably large with and/or without infinite permeability the calculations become complex and has hardly ever been carried out on semi-analytical forms.

In this paper, we develop a linear systematic method called SYSLIMAT Method to facilitate the solution of such complex situations. A series of equations are

developed for the calculations of the magnetic vector potentials and the magnetic scalar potentials from which the flux density can then be easily deduced in different linear media that are separated by concentric cylindrical surfaces. In this study, the number of media can be large. The sources distribution, that can be electric currents and or permanent magnets are carried by any concentric surface, and should be for the study, developed into Fourier's series. The method is then validated through two applications: the study of a classical manual predictable solution and a comparative study of surface permanent magnets synchronous motors (PMSM) with three methods involved, the present method, the magnetic images method, and the use of a numerical code.

II. HYPOTHESIS AND EXPRESSIONS OF POTENTIALS AND FLUX DENSITIES.

II.1 HYPOTHESIS

In this paper the following hypothesis have been considered:

- Two-dimensional system
- Linear homogenous isotropic slot less ferromagnetic media
- Magnetic sources developed into Fourier's series on cylindrical surfaces
- Boundaries on concentric cylindrical surfaces
- Other electric sources also considered on concentric cylindrical surfaces.

The magnetic relative permeability with respect to the flux density $\mu_r(B)$ could be obtained derived from $B(H)$ since the permeability represents the slope of $B(H)$ at any point. The present study consider only constant values of μ_r , further developments of the methods could consider how SYSLIMAT method could help when approaching saturations.

II.2 EXPRESSIONS OF POTENTIALS AND FLUX DENSITIES

In many cases, the electromagnetic study of rotating electrical machines can be simplified by assuming that the boundaries of magnetic materials as well as the sources distributions are cylindrical.

Analytical methods, classically developed [2 -11], suppose that the number of media is small (less than three in general). Some studies have been performed with some difficulties for more than three media [1]. In this paper, a different method is proposed; it is semi-analytical and could be applied to a system with a great number of concentric cylindrical magnetic domains.

The discussed method concerns two-dimensional cylindrical slot less systems with constant magnetic permeability for each involved magnetic media. The concerned media should all then be linear, homogenous and isotropic. The source distributions are developed into Fourier's series. For each rank of a harmonic, the expressions of the magnetic scalar potential, the magnetic vector and the complex magnetic potentials, are then set up, with their unknown coefficients that should be calculated. The relationships between the coefficients are obtained from judicious written forms of boundary conditions.

The originality of our method is the formulation of the last relations under a matrix form which leads to simplifications and makes the method systematic even when there is a very high number of boundaries and media in the models.

The permeability and the geometrical dimensions of the media are expressed under reduced magnitudes. A change of variables permits just one system of equations whichever the position of the studied points with respect to the sources. The properties of diagonal and triangular matrices are used to set the equations on simple matrix forms.

It is known that in one medium, the magnetic charge densities directly lead to magnetic scalar potentials, while the current densities generate vector potentials [1-16]. When considering, in one hand, a medium alone, and in the other hand the same medium with several others, the magnetic potentials created in that medium in both cases are proportional. We can therefore take into account both cases whose sources are magnetic charge density or current density; the expression of the complex magnetic potential can then be employed.

II.1) Calculation of Potentials due to Sources

Let us consider the case of a surface charge density σ^* , on a circular surface of radius R , in a medium of constant magnetic permeability μ (Fig.1). Let σ^* be as follows:

$$\sigma^* = \sigma_o^* \sin v(\theta - \theta_o) \tag{1}$$

Depending on whether $r > R$ or $r < R$, the magnetic scalar potential $V^*(r)$ is given by [2, 3, 4]:

$$V_i^* = -\frac{R}{2v} \sigma^* \left(\frac{r}{R}\right)^v \quad \text{for } r < R \tag{2}$$

$$V_e^* = -\frac{R}{2v} \sigma^* \left(\frac{R}{r}\right)^v \quad \text{for } r > R \tag{3}$$

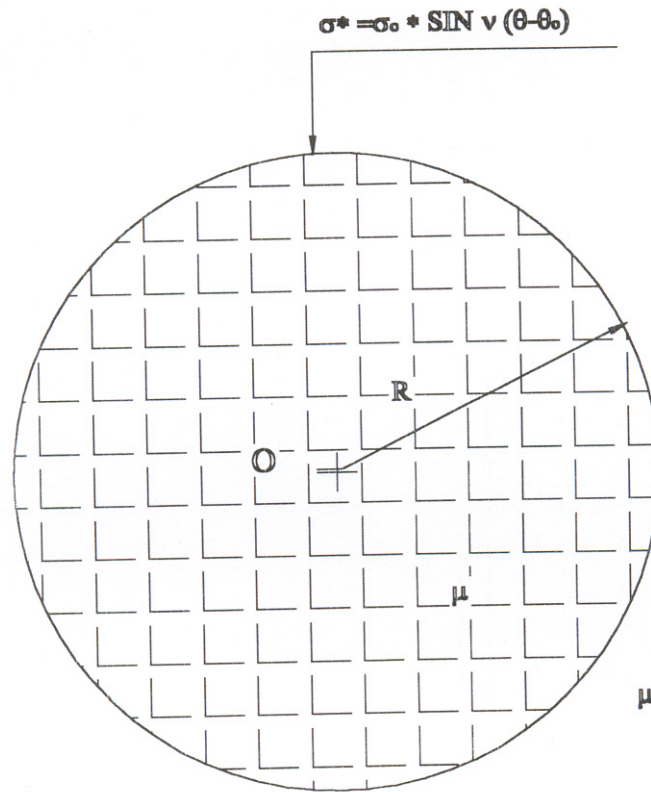


Fig.1 Cylindrical surface of radius R , carrying the magnetic charge density $\sigma^* = \sigma_0^* \sin v(\theta - \theta_0)$ placed in one medium of magnetic permeability μ

Now let a surface current density k be assumed to be present alone on a cylindrical surface of radius R in a medium of constant magnetic permeability μ (Fig.2) and with the expression given as follows:

$$k = K_0 \cos v(\theta - \theta_0) \quad (4)$$

The component $A_z(r)$ of the vector potential with respect to z -axis can be written by the following expressions [2, 3, 4]:

$$A_{zi} = - \frac{R}{2v} \mu K \left(\frac{r}{R} \right)^v \text{ For } r < R \quad (5)$$

$$A_{ze} = - \frac{R}{2v} \mu K \left(\frac{R}{r} \right)^v \text{ For } r > R \quad (6)$$

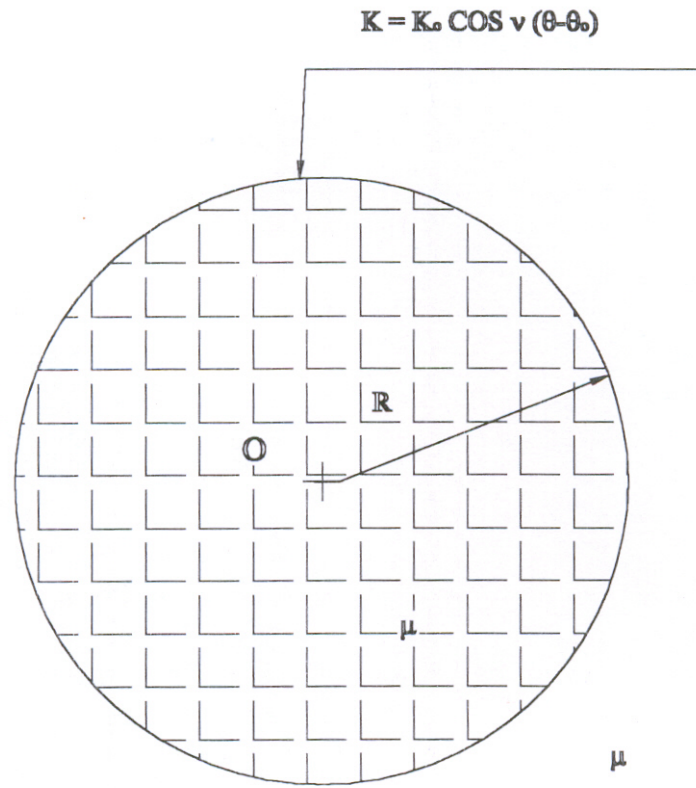


Fig.2 Cylindrical surface of radius R , carrying the magnetic charge density $K = K_0 \cos v(\theta - \theta_0)$ placed in one medium of magnetic permeability μ

II.2) Calculation of Potentials due to the Polarization of Materials

II.2.1) Expressions of potentials and boundary conditions considerations

Let us consider the general case of $k+1$ media, and assume R_k , the radius of the cylinder separating medium k to medium $k+1$, the sources are placed in medium $k+1$, and can be either a current density of expression $k = K_0 \cos v(\theta - \theta_0)$, or a charge density of expression $\sigma^* = \sigma_0^* \sin v(\theta - \theta_0)$, on the surface situated at distance R (Fig.3).

Taking into account the z -axis symmetry of different media, the magnetic scalar potential V_k^* in the medium of index k , will be proportional to $V^*(R)$, when the source is a charge density placed on a surface of radius R . In the same area of index k , the component A_{zk} of the vector potential with respect to z -axis will also be in proportion to $A_z(R)$, if the source is a current density on the same surface of radius R .

$$K = K_0 \cos v(\theta - \theta_0) \text{ or } \sigma^* = \sigma_0^* \sin v(\theta - \theta_0)$$

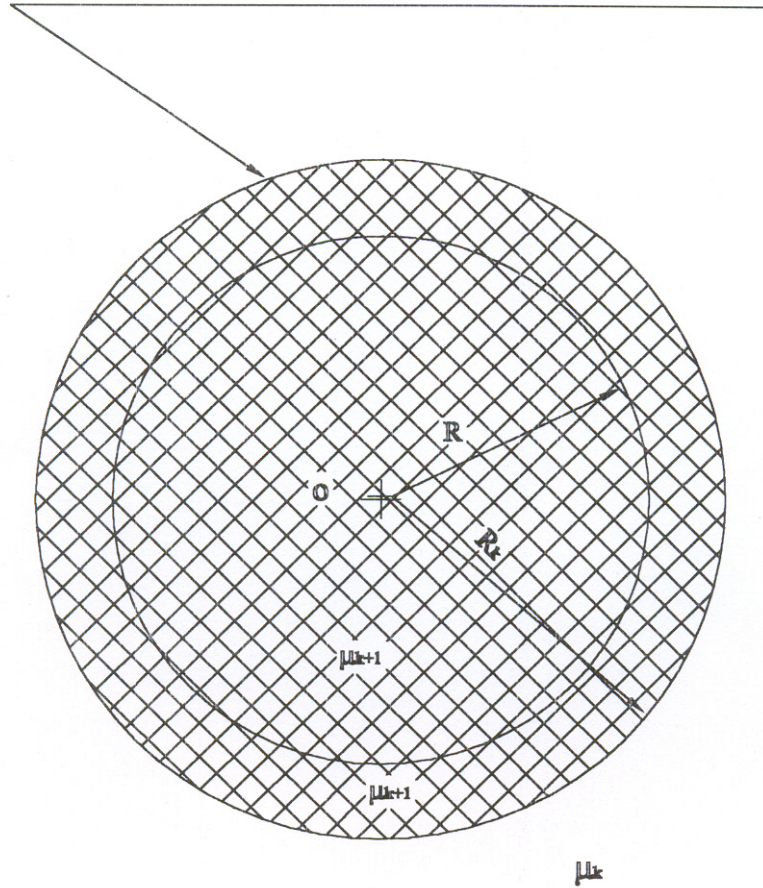


Fig.3 General Case of $k + 1$ media R_k is the radius of the separating surface between the medium $k + 1$ of permeability μ_{k+1} , and the medium k of permeability μ_k . R is the surface placed in the medium $k + 1$, carrying either the current density $K = K_0 \cos v(\theta - \theta_0)$, Or the charge density $\sigma^* = \sigma_0^* \sin v(\theta - \theta_0)$.

In the case where the charge density is considered we have:

$$V_k^* = [a_k \left(\frac{r}{R}\right)^\nu + b_k \left(\frac{R}{r}\right)^\nu] V^*(R) \quad (7)$$

The associated vector potential A_{zk} can be deduced from the above expression. If μ_k is the magnetic permeability of medium k , the complex potential, is written as follows:

$$\Psi_k = A_k + j \mu_k V_k^* \quad (8)$$

Since

$$\Psi_k = [a_k \left(\frac{z}{R}\right)^\nu - b_k \left(\frac{R}{z}\right)^\nu] V^*(R) \quad (9)$$

With

$$z = r \exp j(\theta - \theta_o) \quad (10)$$

It may be noticed that, the associated vector potential is:

$$A_{zk} = \mu_k [a_k \left(\frac{r}{R}\right)^\nu - b_k \left(\frac{R}{r}\right)^\nu] V_k^*(R) \quad (11)$$

- If the source is a current density, A_{zk} should be calculated before, V_k^* can be deduced, therefore we have:

$$A_{zk} = [a_k \left(\frac{r}{R}\right)^\nu + b_k \left(\frac{R}{r}\right)^\nu] A_z(R) \quad (12)$$

$$V_k^* = \frac{1}{\mu_k} [a_k \left(\frac{r}{R}\right)^\nu - b_k \left(\frac{R}{r}\right)^\nu] A_z(R) \quad (13)$$

In all cases, the coefficients a_k and b_k are obtained by applying the boundary conditions between medium k and medium $k+1$. The continuity constraint of A_{zk} and V_k^* can then be written as follows:

- If the source is a charge density, we will have:

$$a_k + b_k \left(\frac{R}{R_k}\right)^{2\nu} = a_{k+1} + b_{k+1} \left(\frac{R}{R_k}\right)^{2\nu} \quad (14)$$

$$\mu_k [a_k - b_k \left(\frac{R}{R_k}\right)^{2\nu}] = \mu_{k+1} [a_{k+1} - b_{k+1} \left(\frac{R}{R_k}\right)^{2\nu}] \quad (15)$$

- If the source is made up by a current density then, we can write:

$$a_k + b_k \left(\frac{R}{R_k}\right)^{2\nu} = a_{k+1} + b_{k+1} \left(\frac{R}{R_k}\right)^{2\nu} \quad (16)$$

$$\frac{1}{\mu_k} [a_k - b_k \left(\frac{R}{R_k}\right)^{2\nu}] = \frac{1}{\mu_{k+1}} [a_{k+1} - b_{k+1} \left(\frac{R}{R_k}\right)^{2\nu}] \quad (17)$$

II.2.2-) Calculation of the coefficients of potentials and the matrices generation

We are then capable to calculate the coefficients of the potentials, and set the matrices generation.

Solutions of (16) and (17) yields:

$$a_k - a_{k+1} = [b_{k+1} - b_k] \left(\frac{R}{R_k}\right)^{2\nu} \quad (18)$$

$$\begin{aligned} & \frac{1}{\mu_k + \mu_{k+1}} [a_k + a_{k+1} - b_k \left(\frac{R}{R_k}\right)^{2\nu} - b_{k+1} \left(\frac{R}{R_k}\right)^{2\nu}] \\ & = \frac{1}{\mu_{k+1} - \mu_k} [a_{k+1} - a_k + b_k \left(\frac{R}{R_k}\right)^{2\nu} - b_{k+1} \left(\frac{R}{R_k}\right)^{2\nu}] \end{aligned} \quad (19)$$

Let us consider:

$$U_k = \frac{\mu_{k+1} + \mu_k}{\mu_{k+1} - \mu_k}$$

$$y = \left(\frac{R}{a}\right)^{2\nu}$$

$$X_k = \left(\frac{a}{R_k} \right)^{2\nu}$$

a: an arbitrary boundary.

Solving (18) and (19) finally gives:

$$a_{k+1} - U_k (b_{k+1} - b_k) y x_k - b_k y x_k = 0 \quad (20)$$

$$a_k - a_{k+1} = [b_{k+1} - b_k] \left(\frac{R}{R_k} \right)^{2\nu} \quad (21)$$

In the case where the source is a charge density, it is sufficient to use $-U_k$ rather than U_k , and we will obtain the corresponding system.

Now let's consider the following situations:

- For $R_k < R$, we will have:

$$a_k = 1 + \alpha_{k-1} \quad (22)$$

$$b_k = \beta_k \quad (23)$$

- And for $R_k > R$, we have:

$$a_k = \alpha_{k-1} \quad (24)$$

$$b_k = 1 + \beta_k \quad (25)$$

So, the system (20) and (21) becomes in both cases:

$$\alpha_k - \alpha_{k-1} = (\beta_{k+1} - \beta_k) y x_k \quad (26)$$

$$\alpha_k - U_k (\beta_{k+1} - \beta_k) y x_k - \beta_k y x_k = V_k \quad (27)$$

With:

$$V_k = -1 \quad \text{if } R_k < R \quad (28)$$

$$V_k = y x_k \quad \text{if } R_k > R \quad (29)$$

Let us consider:

$$\gamma_k = y \beta_k,$$

The system (26) and (27) is then simplified and is reduced to :

$$\alpha_k - \alpha_{k-1} = (\gamma_{k+1} - \gamma_k) x_k \quad (30)$$

$$\alpha_k - U_k x_k (\gamma_{k+1} - \gamma_k) - \gamma_k x_k = V_k \quad (31)$$

Equations 30 and 31 have α_k and γ_k as unknown. In order to solve them, the system is written in matrix form and solved as indicated in the Appendix.

Therefore, all matrices involved in the calculation of α , β , a_k , and b_k , are known.

Let us then in the following sections apply the present proposed method to the studies of some examples that will therefore validate our method.

III. APPLICATION 1: Solution of a Classical Problem.

In order to verify the validity of our method, we've applied it to a classical problem with only two different magnetic zones. The boundary between the media has been supposed equal to a. The source is a current density $k = K_o \cos \nu(\theta - \theta_o)$ on the surface R placed in any of the two media, so we have $R < a$ when the source k is in the medium of magnetic permeability μ_2 , and $R > a$ in the case the source k is in the medium of magnetic permeability μ_1 (Fig.4). The analytical results obtained from the present proposed method are then compared to those obtained by the well known

classical method of magnetic images [3, 16].

Considering the case of two magnetic media (Fig.4), the matrices, α , β , and U are real numbers. We then have:

$$X1 = X = 1$$

$$y = (R/a)^{2v}$$

On the other hand, we have:

$$V = y \quad \text{if } R < a \text{ that is } y < 1$$

$$V = -1 \quad \text{if } R > a \text{ that is } y > 1$$

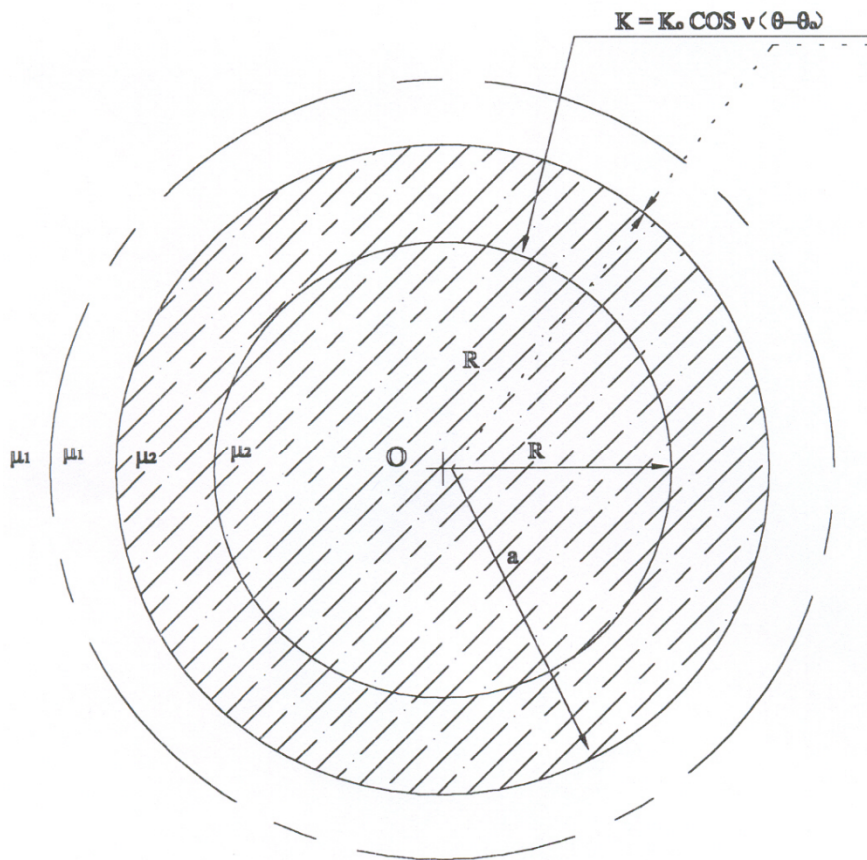


Fig 4.a

	medium 1	medium 2
Permeability	μ_1	μ_2
Coefficient	β	α

(Fig 4.b)

Fig.4a, b Charts of the two media case. The radius of the separating surface is set equal to a. The source is a current density $k = K_0 \cos v(\theta - \theta_0)$ placed in any medium.

In this case $U = (\mu_2 + \mu_1 / \mu_2 - \mu_1)$

It can also be seen that:

$$M = U = \frac{\mu_2 + \mu_1}{\mu_2 - \mu_1} \quad \text{and} \quad M^{-1} = \frac{1}{U}$$

$$\beta = \frac{V}{yU} \quad \text{and} \quad \alpha = \frac{V}{U}$$

These results are summarized in Fig.5.a

To ascertain the validity of this method, the results obtained were compared with that of the classical magnetic image method.

For this reason, the potentials in one medium using the coefficients given on Fig.5.a have been calculated, and the calculation has been repeated making use of the magnetic images method, with the chosen medium suppressed. For example the magnetic potential in the medium 2 must be obtained by suppressing the medium 1. It should be recalled that when a magnetic material is assumed to fill all space, the expressions of the potentials are correct only in the region occupied by that material in the real problem (Figs.5.b, e). We are going to consider a magnetic charge density $\sigma^* = \sigma^*_0 \cos \nu (\theta - \theta_0)$ on R, so $-U$ will be used rather than U , a remains the boundary between the two media of magnetic permeability μ_2 and μ_1 . The image density σ'^* or σ''^* represents the contribution from the suppressed magnetic medium (Figs.5.c, d, f, g). The cylindrical symmetry of the problem (Figs.5.b, e) is such that, on one hand, there is no image in the centre of the concentric cylinders, and on the other hand, the following expressions of the magnetic images σ'^* , σ''^* and of OB, the position of the image σ'^* , are classical, well known [3, 15], and are given below :

$$\sigma'^* = \frac{\mu_1 - \mu_2}{\mu_1 + \mu_2} \sigma^*$$

$$\sigma''^* = \frac{2 \mu_1}{\mu_1 + \mu_2} \sigma^*$$

$$OB = \frac{a^2}{R}$$

Now, we are going to calculate the magnetic potentials V_2^* and V_1^* respectively in the medium of magnetic permeability μ_2 and μ_1 , using on one hand the proposed method presented in this paper, and on the other hand the method of magnetic images. The results obtained will then be compared.

Now, consider the case where $R > a$ (Fig.5.b). The proposed method gives:

-for $r > R$

$$V_1^* = (1 + \beta) \left(\frac{R}{r} \right)^\nu \left(\frac{-R}{2\nu} \right) \sigma^* = \left[1 + \left(\frac{a}{R} \right)^{2\nu} \frac{\mu_1 - \mu_2}{\mu_1 + \mu_2} \right] \left(\frac{R}{r} \right)^\nu \left(\frac{-R}{2\nu} \right) \sigma^*$$

-for $a < r < R$

$$V_1^* = \left[\left(\frac{r}{R} \right)^v + \beta \left(\frac{R}{r} \right)^v \right] \left(\frac{-R}{2v} \right) \sigma^* = \left[\left(\frac{r}{R} \right)^v + \left(\frac{a}{R} \right)^{2v} \frac{\mu_1 - \mu_2}{\mu_1 + \mu_2} \left(\frac{R}{r} \right)^v \right] \left(\frac{-R}{2v} \right) \sigma^*$$

-and for $r < a$

$$V_2^* = (1 + \alpha) \left(\frac{r}{R} \right)^v \left(\frac{-R}{2v} \right) \sigma^* = \left[1 + \frac{\mu_1 - \mu_2}{\mu_1 + \mu_2} \right] \left(\frac{r}{R} \right)^v \left(\frac{-R}{2v} \right) \sigma^*$$

$$= \frac{2 \mu_1}{\mu_1 + \mu_2} \left(\frac{r}{R} \right)^v \left(\frac{-R}{2v} \right) \sigma^*$$

Now considering the equivalent problem obtained by the method of magnetic images (Figs.5.c, d), the equations below are obtained:

-for $r < a$ (Fig.5.c)

$$V_2^* = \left(\frac{r}{R} \right)^v \left(\frac{-R}{2v} \right) \sigma^{*,*} = \left(\frac{r}{R} \right)^v \left(\frac{-R}{2v} \right) \frac{2 \mu_1}{\mu_1 + \mu_2} \sigma^*$$

-for $r > R$ (Fig.5.d)

$$V_1^* = h_1 \left(\frac{R}{r} \right)^v \left(\frac{-R}{2v} \right) \sigma^* + h_2 \left(\frac{OB}{r} \right)^v \left(\frac{-OB}{2v} \right) \sigma^{*,*}$$

-for $a < r < R$ (Fig.5.d)

$$V_1^* = h_3 \left(\frac{r}{R} \right)^v \left(\frac{-R}{2v} \right) \sigma^* + h_4 \left(\frac{OB}{r} \right)^v \left(\frac{-OB}{2v} \right) \sigma^{*,*}$$

Considering that the magnetic potential is discontinuous on $r = R$, as follows:

$$\left\{ \left[\frac{\partial V_1^*}{\partial r} \right]_{r > R} - \left[\frac{\partial V_1^*}{\partial r} \right]_{a < r < R} \right\}_{r=R} = \sigma^*$$

We then find out that:

$$h_1 = h_3 = 1 \text{ and } h_2 = h_4$$

Expressing also that $V_1^*(r=a) = V_2^*(r=a)$ we have:

$$h_4 = \frac{R^2}{a}$$

So the method of magnetic images finally gives:

-for $r < a$

$$V_2^* = \left(\frac{r}{R} \right)^v \left(\frac{-R}{2v} \right) \frac{2 \mu_1}{\mu_1 + \mu_2} \sigma^*$$

-for $r > R$

$$\begin{aligned} \mathbf{V}_1^* &= \left(\frac{\mathbf{R}}{\mathbf{r}}\right)^v \left(\frac{-\mathbf{R}}{2v}\right) \sigma^* + \frac{\mathbf{R}^2}{\mathbf{a}^2} \left(\frac{\mathbf{OB}}{\mathbf{r}}\right)^v \left(\frac{-\mathbf{OB}}{2v}\right) \frac{\mu_1 - \mu_2}{\mu_1 + \mu_2} \sigma^* \\ &= \left[1 + \left(\frac{\mathbf{a}}{\mathbf{R}}\right)^{2v} \frac{\mu_1 - \mu_2}{\mu_1 + \mu_2}\right] \left(\frac{\mathbf{R}}{\mathbf{r}}\right)^v \left(\frac{-\mathbf{R}}{2v}\right) \sigma^* \end{aligned}$$

-for $a < r < R$

$$\begin{aligned} \mathbf{V}_1^* &= \left(\frac{\mathbf{r}}{\mathbf{R}}\right)^v \left(\frac{-\mathbf{R}}{2v}\right) \sigma^* + \frac{\mathbf{R}^2}{\mathbf{a}^2} \left(\frac{\mathbf{OB}}{\mathbf{r}}\right)^v \left(\frac{-\mathbf{OB}}{2v}\right) \frac{\mu_1 - \mu_2}{\mu_1 + \mu_2} \sigma^* \\ &= \left[\left(\frac{\mathbf{r}}{\mathbf{R}}\right)^v + \left(\frac{\mathbf{a}}{\mathbf{R}}\right)^{2v} \frac{\mu_1 - \mu_2}{\mu_1 + \mu_2} \left(\frac{\mathbf{R}}{\mathbf{r}}\right)^v \right] \left(\frac{-\mathbf{R}}{2v}\right) \sigma^* \end{aligned}$$

Finally, in the case where $R > a$, the results obtained by the proposed method are identical to those calculated using the method of magnetic images.

Let's consider the second case where $R < a$, the proposed method gives (Fig.5.e):

-for $r > a$

$$\begin{aligned} \mathbf{V}_1^* &= (1 + \beta) \left(\frac{\mathbf{R}}{\mathbf{r}}\right)^v \left(\frac{-\mathbf{R}}{2v}\right) \sigma^* = \left[1 + \frac{\mu_1 - \mu_2}{\mu_1 + \mu_2}\right] \left(\frac{\mathbf{R}}{\mathbf{r}}\right)^v \left(\frac{-\mathbf{R}}{2v}\right) \sigma^* \\ &= \frac{2\mu_1}{\mu_1 + \mu_2} \left(\frac{\mathbf{R}}{\mathbf{r}}\right)^v \left(\frac{-\mathbf{R}}{2v}\right) \sigma^* \end{aligned}$$

-for $R < r < a$

$$\mathbf{V}_2^* = \left[\alpha \left(\frac{\mathbf{r}}{\mathbf{R}}\right)^v + \left(\frac{\mathbf{R}}{\mathbf{r}}\right)^v \right] \left(\frac{-\mathbf{R}}{2v}\right) \sigma^* = \left[\left(\frac{\mathbf{R}}{\mathbf{a}}\right)^{2v} \frac{\mu_1 - \mu_2}{\mu_1 + \mu_2} \left(\frac{\mathbf{r}}{\mathbf{R}}\right)^v + \left(\frac{\mathbf{R}}{\mathbf{r}}\right)^v \right] \left(\frac{-\mathbf{R}}{2v}\right) \sigma^*$$

-for $r < R$

$$\mathbf{V}_2^* = (1 + \alpha) \left(\frac{\mathbf{r}}{\mathbf{R}}\right)^v \left(\frac{-\mathbf{R}}{2v}\right) \sigma^* = \left[1 + \left(\frac{\mathbf{R}}{\mathbf{a}}\right)^{2v} \frac{\mu_1 - \mu_2}{\mu_1 + \mu_2}\right] \left(\frac{\mathbf{r}}{\mathbf{R}}\right)^v \left(\frac{-\mathbf{R}}{2v}\right) \sigma^*$$

Considering the equivalent magnetic models with the suitable medium suppressed (Figs.5.f, g), we can write:

-for $r > a$ (Fig.5.f)

$$\mathbf{V}_1^* = \left(\frac{\mathbf{R}}{\mathbf{r}}\right)^v \left(\frac{-\mathbf{R}}{2v}\right) \sigma^{*,*} = \left(\frac{\mathbf{R}}{\mathbf{r}}\right)^v \left(\frac{-\mathbf{R}}{2v}\right) \frac{2\mu_1}{\mu_1 + \mu_2} \sigma^*$$

-for $r < R$ (Fig.5.g)

$$V_2^* = h_7 \left(\frac{r}{R} \right)^v \left(\frac{-R}{2v} \right) \sigma^* + h_8 \left(\frac{r}{OB} \right)^v \left(\frac{-OB}{2v} \right) \sigma^*$$

-for $R < r < a$

$$V_2^* = h_9 \left(\frac{R}{r} \right)^v \left(\frac{-R}{2v} \right) \sigma^* + h_{10} \left(\frac{r}{OB} \right)^v \left(\frac{-OB}{2v} \right) \sigma^*$$

Noticing also that the magnetic potential is discontinuous on the surface $r = R$, the following equation is obtained:

$$\left\{ \left[\frac{\partial V_2^*}{\partial r} \right]_{R < r < a} - \left[\frac{\partial V_2^*}{\partial r} \right]_{r < R} \right\}_{r=R} = \sigma^*$$

We then find out that:

$$h_7 = h_9 = 1 \text{ and } h_8 = h_{10}$$

Also considering here the continuity of the magnetic potential on $r = a$, that is $V_1^*(r=a) = V_2^*(r=a)$, we got:

$$h_{10} = \frac{R^2}{a^2}$$

So the magnetic image method finally gives in the above case the following equations ($R < a$):

-for $r > a$

$$V_1^* = \left(\frac{R}{r} \right)^v \left(\frac{-R}{2v} \right) \frac{2 \mu_1}{\mu_1 + \mu_2} \sigma^*$$

-for $R < r < a$

$$\begin{aligned} V_2^* &= \left(\frac{R}{r} \right)^v \left(\frac{-R}{2v} \right) \sigma^* + \frac{R^2}{a^2} \left(\frac{r}{OB} \right)^v \left(\frac{-OB}{2v} \right) \frac{\mu_1 - \mu_2}{\mu_1 + \mu_2} \sigma^* \\ &= \left[\left(\frac{R}{a} \right)^{2v} \frac{\mu_1 - \mu_2}{\mu_1 + \mu_2} \left(\frac{r}{R} \right)^v + \left(\frac{R}{r} \right)^v \right] \left(\frac{-R}{2v} \right) \sigma^* \end{aligned}$$

-and for $r < R$

$$\begin{aligned} V_2^* &= \left(\frac{r}{R} \right)^v \left(\frac{-R}{2v} \right) \sigma^* + \frac{R^2}{a^2} \left(\frac{r}{OB} \right)^v \left(\frac{-OB}{2v} \right) \frac{\mu_1 - \mu_2}{\mu_1 + \mu_2} \sigma^* \\ &= \left[1 + \left(\frac{R}{a} \right)^{2v} \frac{\mu_1 - \mu_2}{\mu_1 + \mu_2} \right] \left(\frac{r}{R} \right)^v \left(\frac{-R}{2v} \right) \sigma^* \end{aligned}$$

Finally, in this case ($R > a$), the results obtained by both the proposed method and the method of magnetic images are identical.

It can then be drawn the general conclusion that in the case of two magnetic media (Fig.5.a, b, e), this proposed method and the classical method of magnetic images both lead to the same results.

	α	β
$R < a$	y/U	$1/U$
$R > a$	$-1/U$	$-1/(y U)$

(Fig.5a)

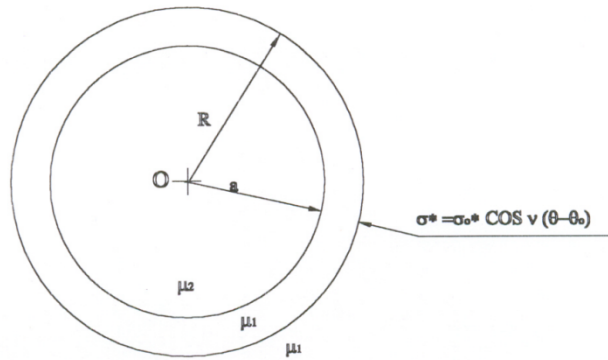


Fig. 5 b

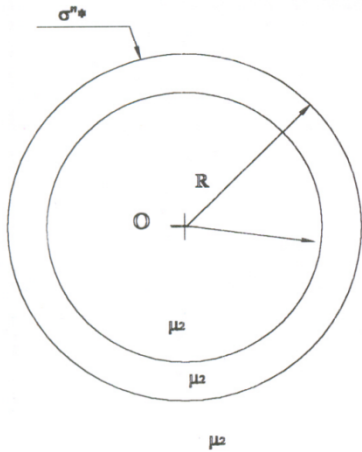


Fig.5.c

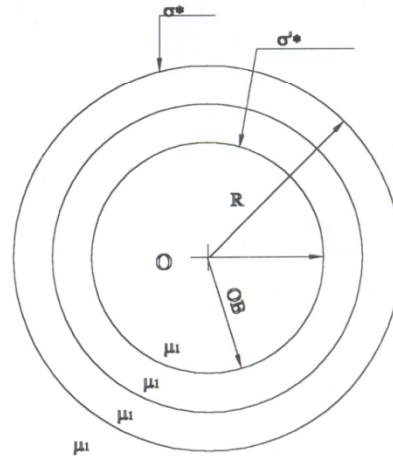
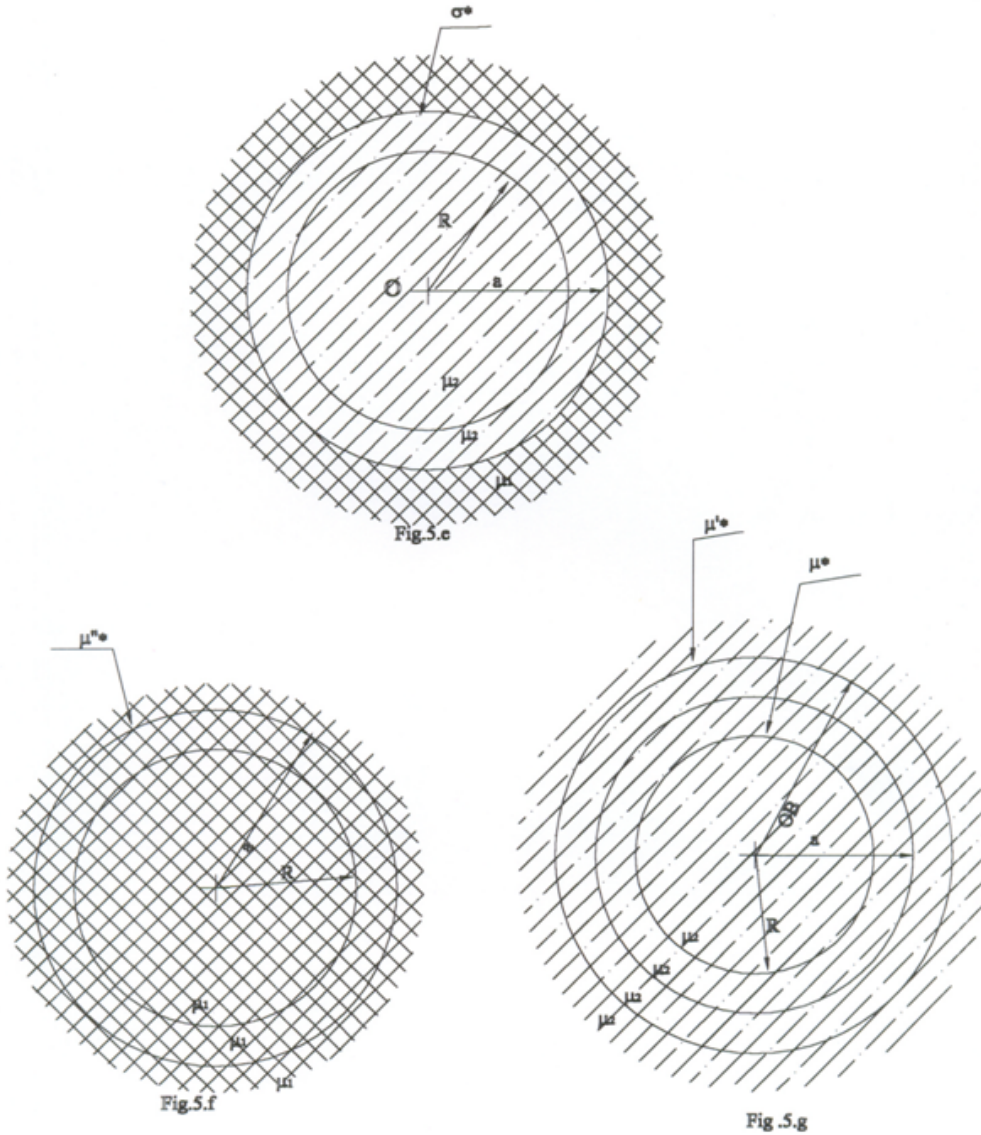


Fig.5.d

Figs.5.a, b, c, d: (a) Coefficients α and β in the two media case (b) Two media case with $R > a$. a is the boundary between the media. The source is a magnetic charge density σ^* on R . (c) Magnetic image in the case $R > a$ with the medium 2 assumed to fill All space (the medium 1 is suppressed) (d) Magnetic image in the case $R > a$ with the medium 1 assumed to fill All space (the medium 2 is suppressed)



Figs.5.e, f, g: (e) Two media case with $R < a$, a is the boundary between the media. The source is a magnetic charge density σ^* on R . (f) Magnetic image in the case $R < a$ with the medium 1 assumed to fill all Space (the medium 2 is suppressed) (g) Magnetic image in the case $R < a$ with the medium 2 assumed to fill all Space (the medium 1 is suppressed)

IV.) APPLICATION 2: on the study of a Radial Permanent Magnet Synchronous Motor – Comparison with other analytical and numerical methods
IV.1 Application to the design of the excitation of a Radial Permanent Magnet Synchronous

The calculation of the flux density in a slot less sector-shaped permanent magnet synchronous machine is also carried out as a second application of the proposed

method. The results are favourably compared to those obtained in previous papers [11-16]. In order to approach a real motor, an analytical model with finite values of the permeability is developed.

The machines studied here are supposed to be sufficiently long and hold permanent magnets with surface radial magnetizations and without polar pieces. So the system can be considered as two-dimensional (Fig.6a), and slot less. The permanent magnets that can be used here could be the followings:

- NdFeB with $B_r(R) = 1.2T$; $H_c = 900$ A/m; $\mu_r = 1.05$
- SmCo₁₇ with $B_r(R) = 1.07T$; $H_c = 720$ A/m; $\mu_r = 1.05$
- Ferrites with $B_r(R) = 0.39T$; $H_c = 230$ A/m; $\mu_r = 1.01$

All those rare earth magnets generally present linear demagnetization characteristics, with $B_r(R) = M_{rad}(R)$ inside the magnets when the magnetic field is zero.

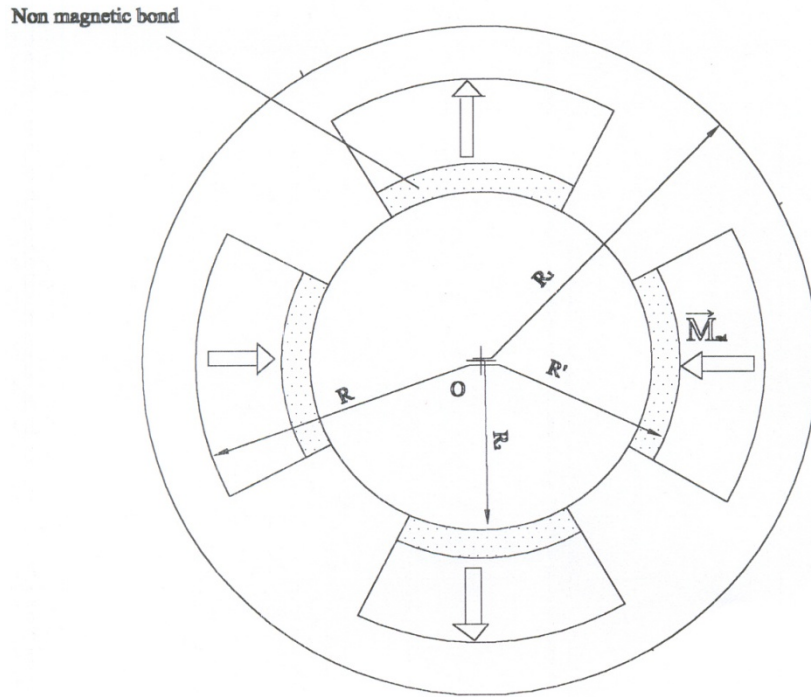


Fig. 6.a

medium (1)	medium (2)	medium (3)
stator	real air gap and the magnets	rotor

(Fig.6b)

Fig.6a, b The structure of a real 4-poles PMSM. Only the interior radius R_1 of the stator is considered. R' and R are respectively, the interior and the exterior radius of the permanent magnets. R_2 is the radius of the rotor. θ_{ra} is the half aperture of the magnets. The system is described counter clockwise. (R' and R_2 are here different, but the method allows taking them equal)

As we have seen above, the magnets used in the studied Permanent Magnets Synchronous Machines, are rare earth types. Since they have linear demagnetization characteristics with high coercive fields H_c , they cannot be easily demagnetized while running. Let's notice also that they have approximately $\mu_r = 1$ and radial magnetization \vec{M}_{rad}

So, using the expression, $\vec{B} = \mu_o \vec{H} + \vec{M}_{rad}$ rather than $\vec{B} = \mu_o \left(\vec{H} + \vec{M}_{rad} \right)$, [16], we have M_{rad}

in Tesla, and considering that inside a magnet the flux density is conserved between two surfaces of the same differential angle $d\theta$, with one surface on r and the other on R , we can write:

$$M_{rad}(r) r d\theta = M_{rad}(R) R d\theta$$

So, $M_{rad}(r)$ varies as $1/r$, therefore:

$$M_{rad}(r) = M_{rad}(R) R/r$$

We know that according to Coulomb's model, the magnetic scalar potential V^* created in the air gap by the permanent magnets of magnetization \vec{M}_{rad} , (Fig 6.c), is the same as the one generated by the volume charge densities ρ^* and the surface charge density σ^* with:

$$\rho^* = - \text{div } \vec{M}_{rad}$$

$$\sigma^* = \vec{M}_{rad} \cdot \vec{n}$$

\vec{n} : being the exteriorly oriented normal vector at the surface of the magnets.

Since the magnets used in our study have the characteristics described above with \vec{M}_{rad} varying in $1/r$, $\text{div } \vec{M}_{rad} = 0$, so the volume charge densities ρ^* can be neglected, and only the surface charge densities σ^* could be considered. The sources can then be modelled as follows (Fig 6.c):

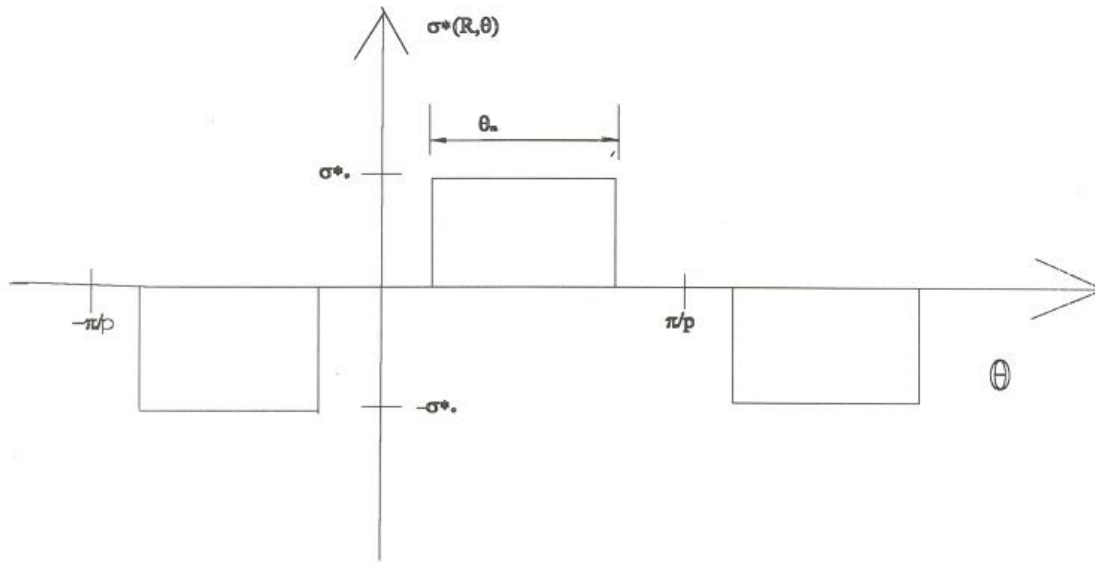


Fig.6c Representation of the equivalent charge densities on the surface of radius R with respect to the angle θ

So we have:

$$\sigma^*(R, \theta) = \sigma_0^* \sum_{n=0}^{\infty} b_n \sin \nu \theta$$

$$\sigma^*(R', \theta) = -\frac{R}{R'} \sigma^*(R, \theta)$$

With:

$$b_n = (-1)^n \left(\frac{4p}{\nu \pi} \right) \sin \nu \theta_{ra}$$

$$\nu = (2n + 1)p$$

θ_{ra} : the half aperture of the magnets

The magnets can then be replaced by the concentric charged surfaces with the charge densities $\sigma^*(R, \theta)$, $\sigma^*(R', \theta)$ on, the stator and the rotor remaining unchanged.

Having justified the representation of the permanent magnets, the following general analytical model can be considered.

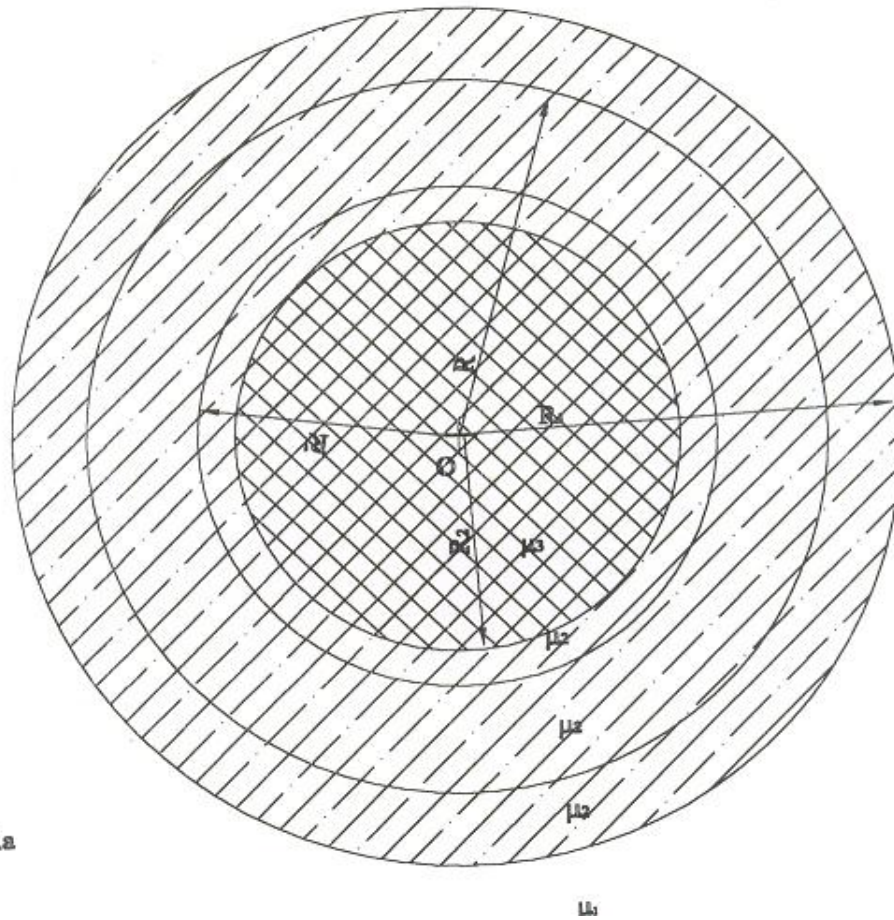


Fig. 7.a

	medium (1)	medium (2)	medium (3)
Permeability	μ_1	$\mu_2 = \mu_0$	μ_3
Coefficients	$0, 1 + \beta_1$	- for $r > R : \alpha_1, 1 + \beta_2$ - for $r < R : 1 + \alpha_1, \beta_2$	$1 + \alpha_2, 0$

(Fig.7b)

Figs.7a, b General analytical model of the PMSM. The sources are the charge densities $\sigma^*(R, \theta)$ and $\sigma^*(R', \theta)$ on the concentric surfaces of radii R and R' . The medium2 is the magnetic air gap made up by the magnets and the real air gap, it has the permeability μ_0 . The coefficients in each region are given.

It comes out that three media are involved here, with two boundaries. So the matrices M and Q have two rows and two columns. In general, we have, regardless of the positions of the sources:

$$M = \begin{bmatrix} U_1 X_1 & -(U_1 + 1) X_1 \\ X_1 & U_2 X_2 - X_1 \end{bmatrix}$$

We can then set:

$$z = \frac{1}{y} \quad \text{and} \quad a = R_1 \quad \text{thus} \quad X_1 = 1 \quad \text{and} \quad X_2 = X = \left(\frac{R_1}{R_2}\right)^{2\nu}$$

With:

$$y = \left(\frac{R}{R_1}\right)^{2\nu}$$

The following results are obtained:

$$\beta = \frac{z}{1 + U_1 U_2 X} \begin{bmatrix} U_2 X^{-1} & 1 + U_1 \\ -1 & U_1 \end{bmatrix} \begin{bmatrix} V_1 \\ V_2 \end{bmatrix}$$

$$\alpha = \frac{1}{1 + U_1 U_2 X} \begin{bmatrix} 1 & -1 \\ 1 & X - 1 \end{bmatrix} \begin{bmatrix} U_2 X^{-1} & 1 + U_1 \\ -1 & U_1 \end{bmatrix} \begin{bmatrix} V_1 \\ V_2 \end{bmatrix}$$

Three different expressions of the vector V arises depending on the position of the source. They are summarized in the following table (Fig.8).

	V ₁	V ₂
R > R ₁	-1	-1
R ₂ < R < R ₁	Y	-1
R < R ₂	Y	Y X

Fig.8 Different values of the vector V in the three media case

Usually, the relative permeability of the iron parts (the rotor and the stator), is greater (in a very high ratio), than those of the air gap and the magnets. Therefore, they have been considered in this paper to be infinite.

In previous papers [11-16], the magnetic scalar potentials have been calculated in the magnetic air gap, using the method of the separation of variables in Laplace's equations, those having infinite permeability (i.e. The iron parts) (Fig.7a, b). It has been found:

For R₂ < r < R

$$V_1^* = \sum_{n=0}^{\infty} \left[c_n \left(\frac{r}{R}\right)^{\nu} + d_n \left(\frac{R}{r}\right)^{\nu} \right] \sin \nu \theta$$

For R < r < R₁

$$V_2^* = \sum_{n=0}^{\infty} \left[f_n \left(\frac{r}{R}\right)^{\nu} + g_n \left(\frac{R}{r}\right)^{\nu} \right] \sin \nu \theta = \sum_{n=0}^{\infty} \left[g_n \left(\frac{r}{R}\right)^{\nu} + d_n \left(\frac{R}{r}\right)^{\nu} \right] \left(\frac{S_b}{2}\right) V^*(R)$$

With:

$$f_n = \frac{\left[1 - \left(\frac{R_2}{R} \right)^{2\nu} \right] \left(\frac{S_b}{2} \right)}{\left(\frac{R_2}{R} \right)^{2\nu} - \left(\frac{R_1}{R} \right)^{2\nu}}$$

$$g_n = - f_n \left(\frac{R_1}{R} \right)^{2\nu}$$

$$c_n = f_n + \left(\frac{S_b}{2} \right)$$

$$d_n = g_n - \left(\frac{S_b}{2} \right)$$

$$S_b = \sigma_0^* R \left(\frac{b_n}{\nu} \right)$$

It will be shown hereafter that the present proposed method leads to the same expressions of V_1^* and V_2^* . When μ_1 and μ_2 approach infinity, U_1 and U_2 respectively tend to -1 and 1, α_k and β_k are then:

$$\alpha_1 = \frac{XV_1 + V_2}{1 - X} \quad \beta_1 = -zV_1$$

$$\alpha_2 = V_2 \quad \beta_2 = -z \frac{V_1 + V_2}{1 - X}$$

The magnetic source being assumed in the medium 2, we then have:

$$V_1 = y \text{ and } V_2 = -1$$

Therefore:

$$\alpha_1 = \frac{Xy - 1}{1 - X} \quad \beta_1 = -1$$

$$\alpha_2 = -1 \quad \beta_2 = -z \frac{y - 1}{1 - X}$$

This leads to:

$$\alpha_1 = \frac{\left(\frac{R}{R_2} \right)^{2\nu} - 1}{1 - \left(\frac{R_1}{R_2} \right)^{2\nu}} \quad \beta_1 = -1$$

$$\alpha_2 = -1 \quad \beta_2 = \frac{\left(\frac{R_1}{R} \right)^{2\nu} - 1}{1 - \left(\frac{R_1}{R_2} \right)^{2\nu}}$$

If the position of the studied points is between the concentric surfaces of radii R and R_1 , the coefficients to be considered are α_1 and $1 + \beta_2$

For points located between R_2 and R , the coefficients $1 + \alpha_1$ and β_2 must be used.

It can be verified that $b_1 = 1 + \beta_1$ and $a_2 = 1 + \alpha_2$ both tend to zero as μ_1 and μ_2 approach infinity.

So supposing the studied point being located between R and R_1 , the magnetic scalar potential is given by:

$$V_2^* = \left[\alpha_1 \left(\frac{r}{R} \right)^\nu + (1 + \beta_2) \left(\frac{R}{r} \right)^\nu \right] V^*(R)$$

The following results are then obtained:

$$g_n = \alpha_1 \text{ and } d_n = 1 + \beta_2$$

Therefore, the expressions of V_2^* in both cases, are equivalent. It is easy to carry out the same demonstration for V_1^* .

We can then conclude that both methods lead to the same results, the present proposed method being henceforth validated.

The flux density in any medium can then generally be deduced from the form of the magnetic scalar potential (Eq.7). So, the expressions of the magnetic scalar potentials and those of the radial components of the flux density can be written for medium k , outside the magnet domains as follows:

$$\begin{aligned} V_k^*(r, \theta) = & \sum_{n=0}^{\infty} \left[a_k \left(\frac{r}{R} \right)^\nu + b_k \left(\frac{R}{r} \right)^\nu \right] \frac{(-\sigma_0^* R)}{2\nu} \sin \nu \theta \\ & + \sum_{n=0}^{\infty} \left[a'_k \left(\frac{r}{R'} \right)^\nu + b'_k \left(\frac{R'}{r} \right)^\nu \right] \frac{(-\sigma_0^* R')}{2\nu} \sin \nu \theta \end{aligned}$$

And

$$\begin{aligned} B_r(r, \theta) = & \sum_{n=0}^{\infty} \left[a_k \left(\frac{r}{R} \right)^\nu - b_k \left(\frac{R}{r} \right)^\nu \right] \frac{(-\sigma_0^* R)}{2\nu} \sin \nu \theta \\ & + \sum_{n=0}^{\infty} \left[a'_k \left(\frac{r}{R'} \right)^\nu - b'_k \left(\frac{R'}{r} \right)^\nu \right] \frac{(-\sigma_0^* R')}{2\nu} \sin \nu \theta \end{aligned}$$

The coefficients a_k and b_k depend on the source placed at R , when a'_k and b'_k have their origin in the source situated at R' . All these coefficients are calculated using the proposed systematic matrix method (Eqs.46, 45, 44, 38, 37, 36, 23, 22).

Computing the expressions of the radial component of the flux density (B_r), we can practically set $\mu_1 = 1000$, $\mu_2 = 1$, $\mu_3 = 1000$, which implies μ_1 and μ_3 greater in a very high ratio, than μ_2 , the method offering anyway the possibility of calculating B_r in the iron parts (Figs.6a, b). We found out with a 3% error, almost the same results as in [11, 12], the studied points being $r_1 = 8.6\text{cm}$, $r_2 = 7.5\text{cm}$ and $r_3 = 5\text{cm}$, respectively in the medium 1, 2, and 3 (Figs.10, a, b, c), and when putting the spot in the air gap of the permanent magnets synchronous motor, the surfaced magnets being carried by the rotor and the stator assumed slot less, we obtained the results on figures 10, d, e, and

f, which are validated by a comparative study with three different methods involved.

On the other hand, using the above general expressions of V_k^* and corresponding deduced B_r , the sources remaining at the same positions R and R', more than three media can be examined (Figs.7a, b). We then have considered the case where the external radius of the stator is finite, the medium outside the machine being the air. It should be pointed that this method offers the possibility to also study the case where the mass of the magnetic materials is optimised, e.g. a case where a cylindrical concentric hole is considered in the rotor part of the same PMSM. Five magnetic media have to be considered in this specific case of optimising the mass of the system.

Having taken into account four media: the solid rotor, the magnetic air gap, the stator, and the air outside the machine, the flux densities in the iron parts and the air gap have been calculated at the same positions as in the case of three media, that is at the positions $r_2 = 8.6\text{cm}$, $r_3 = 7.5\text{cm}$ and $r_4 = 5\text{cm}$, in respectively the stator, the air gap, and the rotor, but with the permeability of the irons chosen to approach a real case: $\mu_1 = 1$, $\mu_2 = 10$ $\mu_3 = 1$, and $\mu_4 = 10$ (Figs.11a, b, c, d).

We can see that the flux densities in the irons are still weak, while the magnetic losses made up by field lines outside the machine, that is in the medium 1, can be neglected, the points studied being at the position $r_1 = 15\text{cm}$.

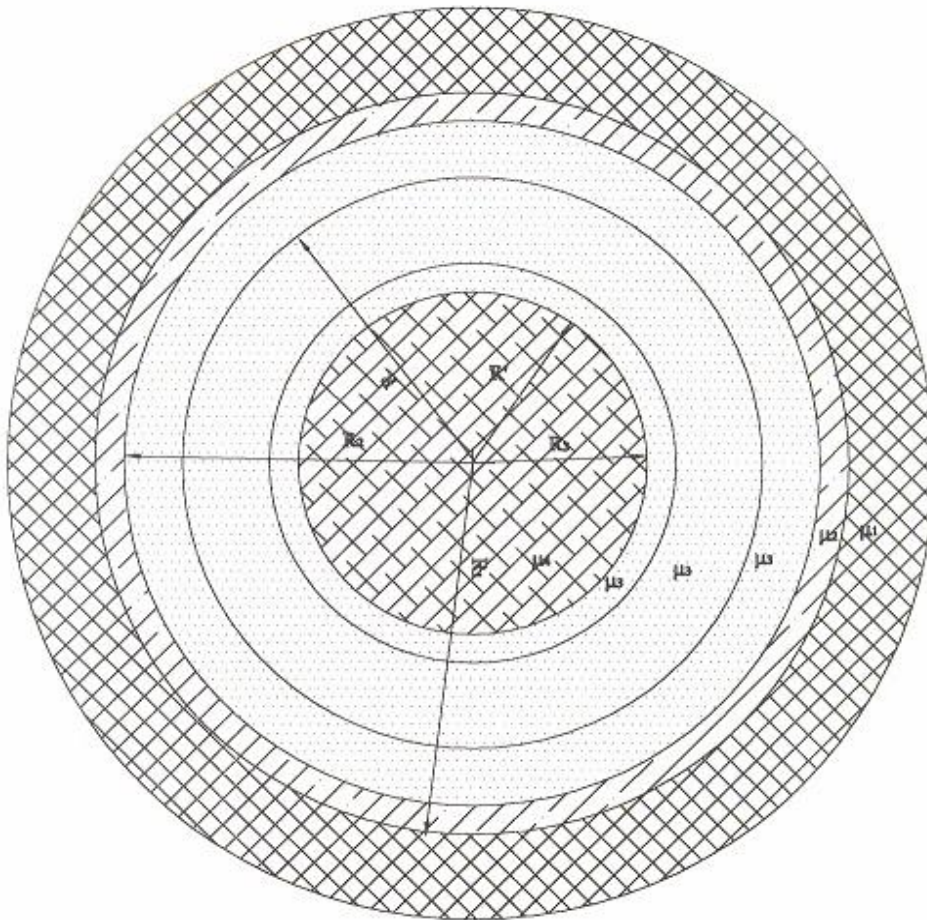
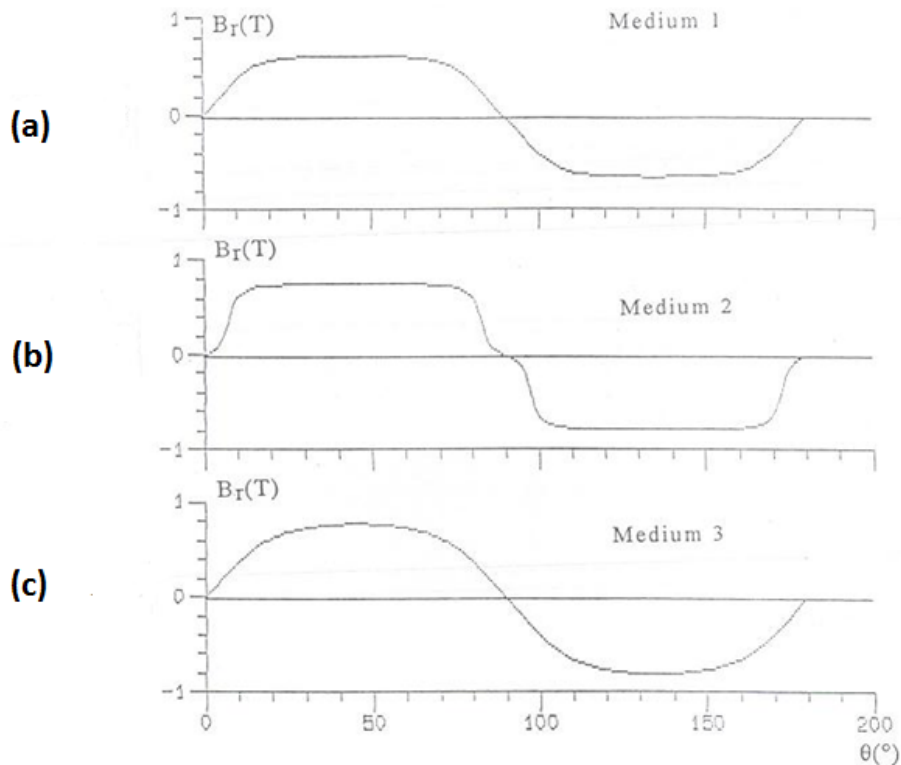


(Fig.9a)

	medium (1)	medium (2)	medium (3)	medium (4)
Name	air (outside of the machine)	Stator	Magnetic air gap (real air gap + magnets)	Rotor
Permeability	$\mu_1 = \mu_0$	μ_2	$\mu_3 = \mu_0$	μ_4
Coefficients	$0, 1 + \beta_1$	$\alpha_1, 1 + \beta_2$	- for $r > R$: $\alpha_2, 1 + \beta_3$ - for $r < R$: $1 + \alpha_2, \beta_3$	$1 + \alpha_3, 0$

(Fig.9b)

Figs.9a, b: Representation of the analytical model of the PMSM with the outside of the machine considered. The case involves four media. R_1 and R_2 are respectively the external and the interior radius of the stator. R' and R are the surfaces carrying the sources. R_3 is the radius of the rotor. The medium 3 is the magnetic air gap made up by the magnets and the real air gap, it has the permeability μ_0 . The coefficients in each region are given.



Figs 10.a, b, c: Graphs of the radial components of the flux densities in the studied PMSM. The permeability of the iron parts are supposed finite. Three media are considered.

The Machine Data :

$p = 2$ $R_1 = 8.29\text{cm}$ $R_2 = 6.48\text{cm}$ $R = 7.23\text{cm}$

$R' = 6.5\text{cm}$ $\mu_1 = 1000$ $\mu_2 = 1$ $\mu_3 = 1000$

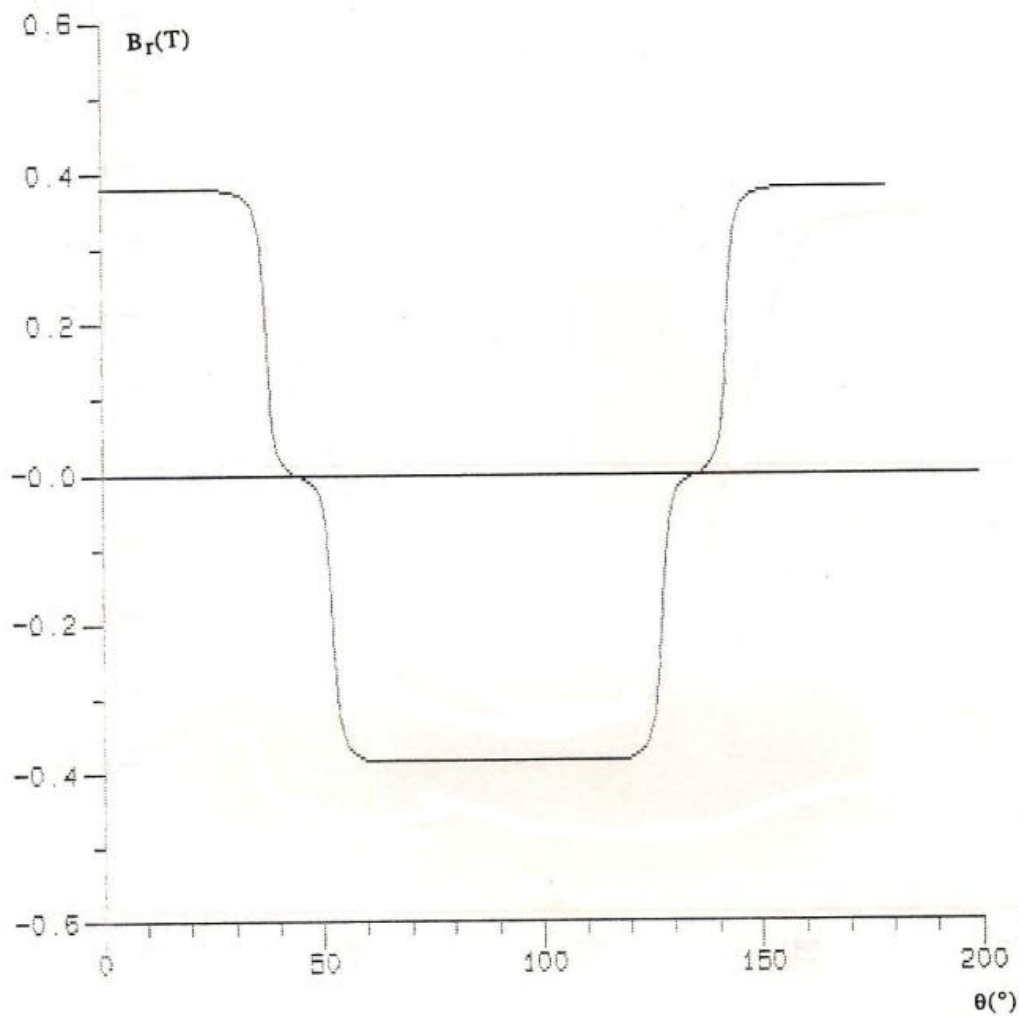
$2\theta_{ra} = 75^\circ$

The Studied Points:

$r_1 = 8.6\text{cm}$ in the medium 1

$r_2 = 7.5\text{cm}$ in the medium 2

$r_3 = 5\text{cm}$ in the medium 3



Figs 10.d: Radial Component of the flux density generated by permanent magnet in the air gap. The permeability of the iron parts are supposed finite. Three media are considered.

The Machine Data :

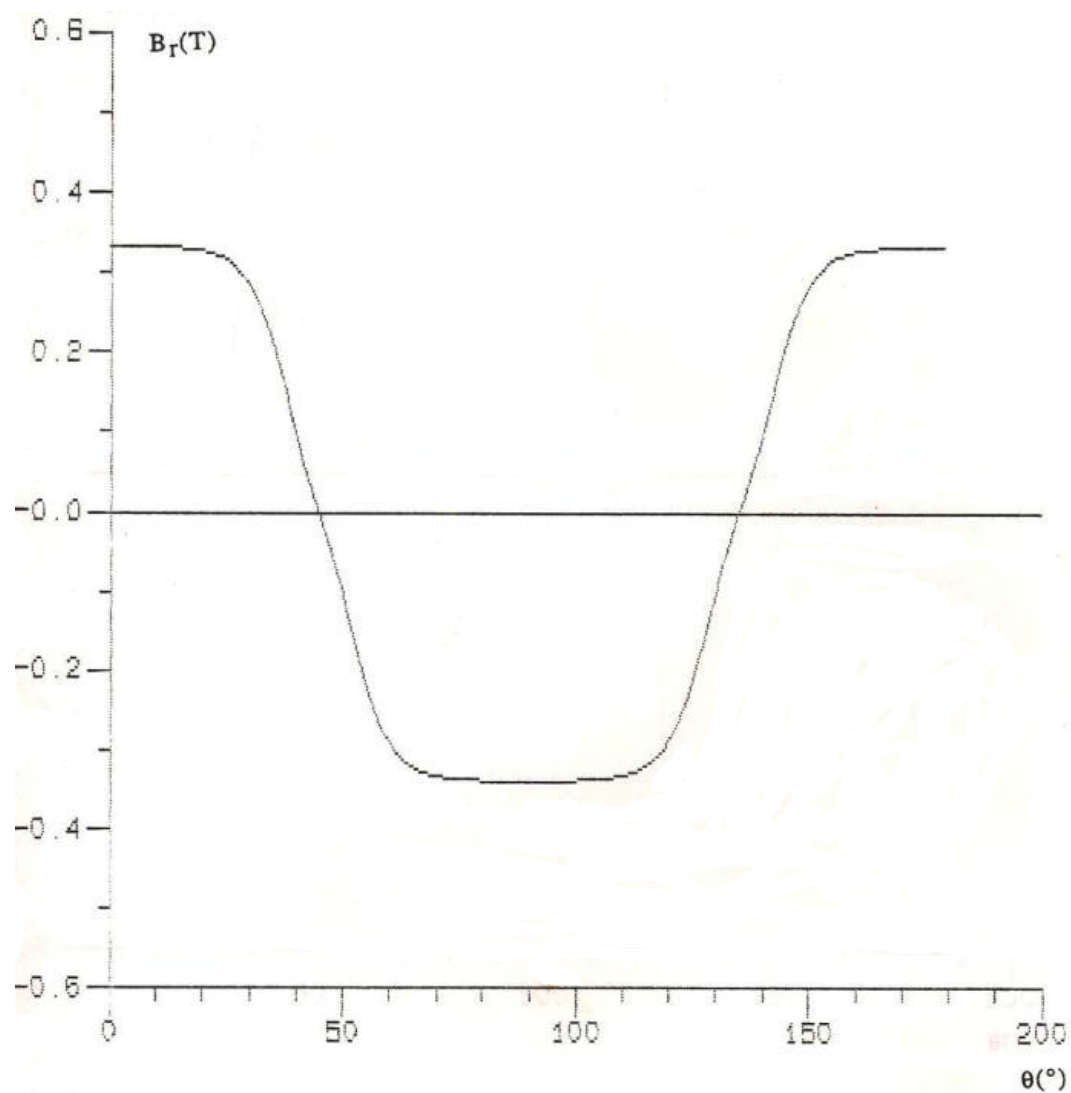
$$p = 2 \quad R_1 = 8.39\text{cm} \quad R_2 = 6.48\text{cm} \quad R = 7.23\text{cm}$$

$$R' = 6.48 \text{ cm} \quad \mu_1 = 1000 \quad \mu_2 = 1 \quad \mu_3 = 1000$$

$$2\theta_{ra} = 75^\circ \quad \mu_0 \quad M = 0.92 \text{ T (NdFeB)}$$

The Studied Points:

$r = 7.38 \text{ cm}$ in the air gap



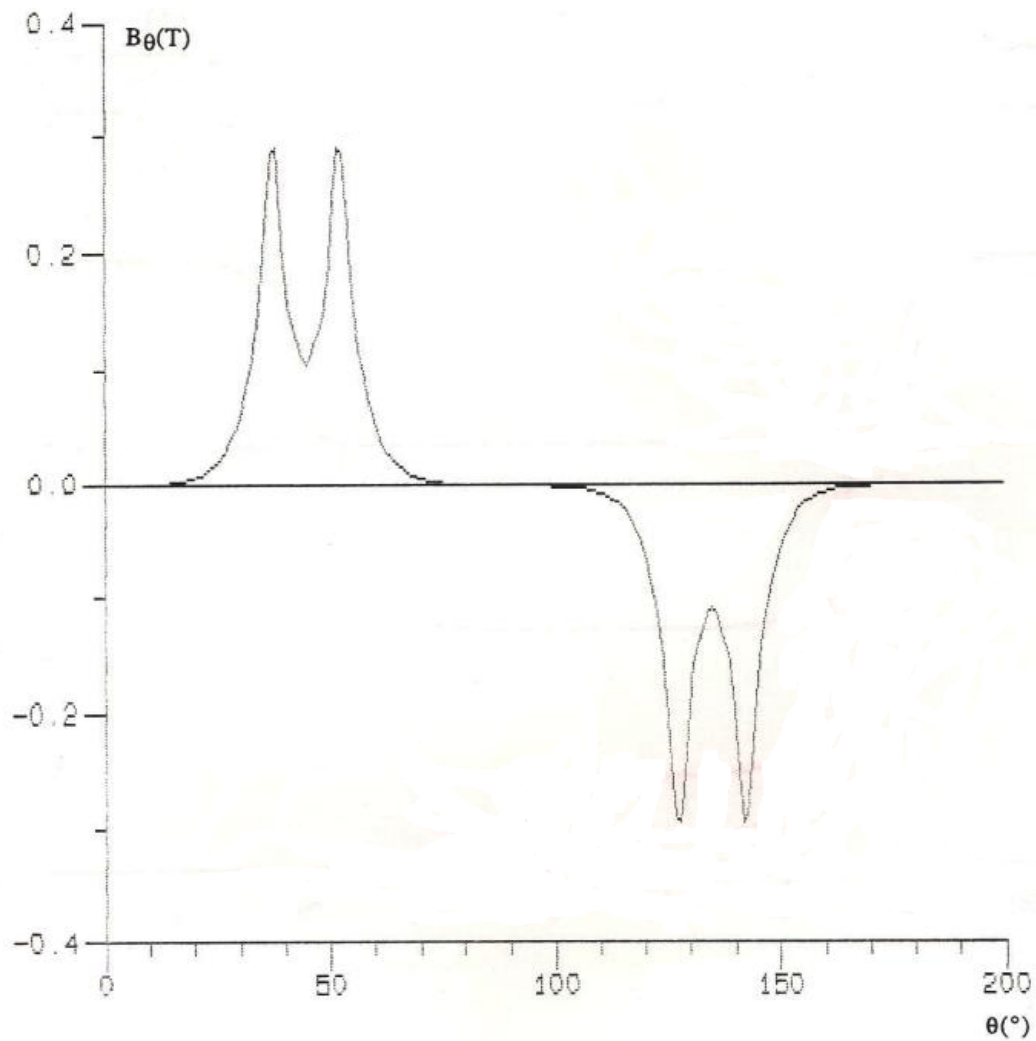
Figs 10.e: Radial Component of the flux density generated by permanent magnet at the interior surface of the stator. The permeability of the iron parts are supposed finite. Three media are considered.

The Machine Data :

$p = 2$ $R_1 = 8.39\text{cm}$ $R_2 = 6.48\text{cm}$ $R = 7.23\text{cm}$
 $R' = 6.48\text{ cm}$ $\mu_1 = 1000$ $\mu_2 = 1$ $\mu_3 = 1000$
 $2\theta_{ra} = 75^\circ$ $\mu_0 M = 0.92\text{ T}$ (NdFeB)

The Studied Points:

$r = 8.39\text{cm}$ on the interior surface of the stator



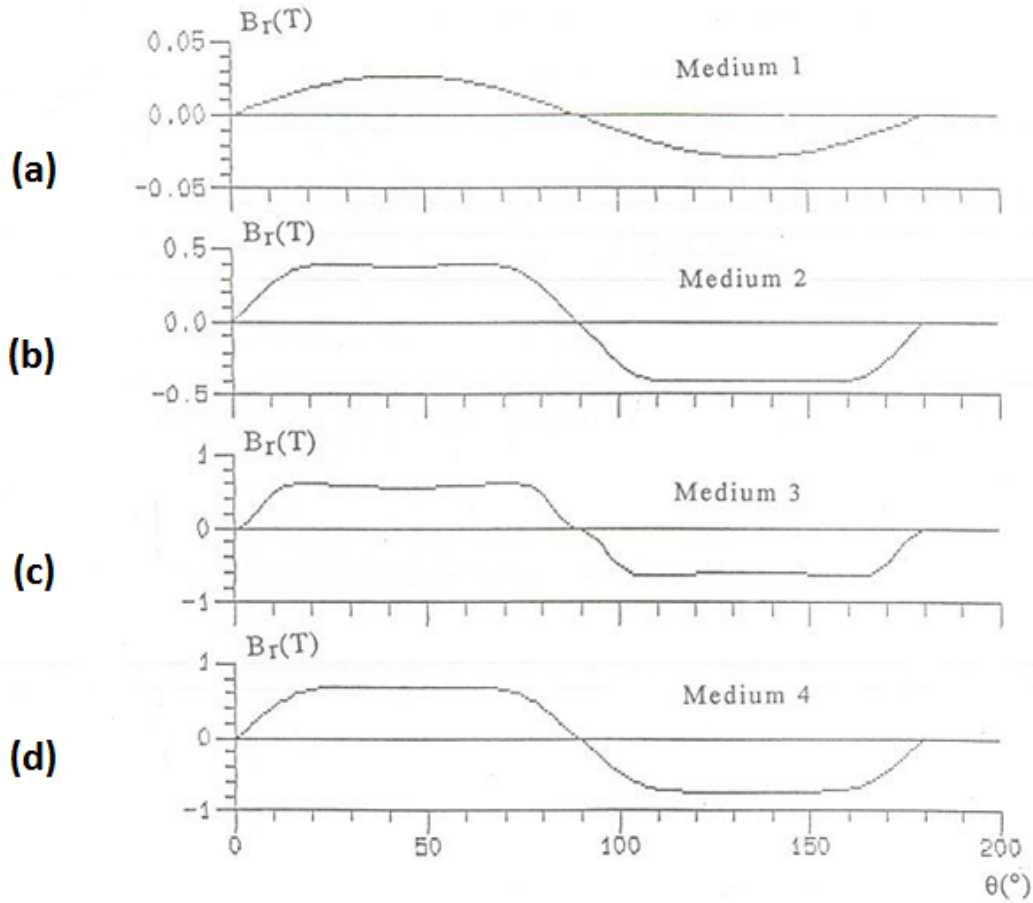
Figs 10.f: Tangential Component of the flux density generated by permanent magnet in the air gap. The permeability of the iron parts are supposed finite. Three media are considered.

The Machine Data :

$p = 2$ $R_1 = 8.39\text{cm}$ $R_2 = 6.48\text{cm}$ $R = 7.23\text{cm}$
 $R' = 6.48\text{ cm}$ $\mu_1 = 1000$ $\mu_2 = 1$ $\mu_3 = 1000$
 $2\theta_{ra} = 75^\circ$ $\mu_0 M = 0.92\text{ T}$ (NdFeB)

The Studied Points:

$r = 7.38$ cm in the air gap



Figs 11.a, b, c, d: Graphs of the radial components of the flux densities in the studied PMSM. The permeability of the iron parts is assumed finite. Four media are considered.

The Machine Data:

$p = 2$ $R_1 = 10$ cm $R_2 = 8.29$ cm $R_3 = 6.48$ cm

$R = 7.23$ cm $R' = 6.5$ cm $\mu_1 = 1$ $\mu_2 = 10$

$\mu_3 = 1$ $\mu_4 = 10$ $2\theta_{ra} = 75^{\circ}$

The Studied Points:

$r_1 = 15$ cm in the medium 1

$r_2 = 8.6$ cm in the medium 2

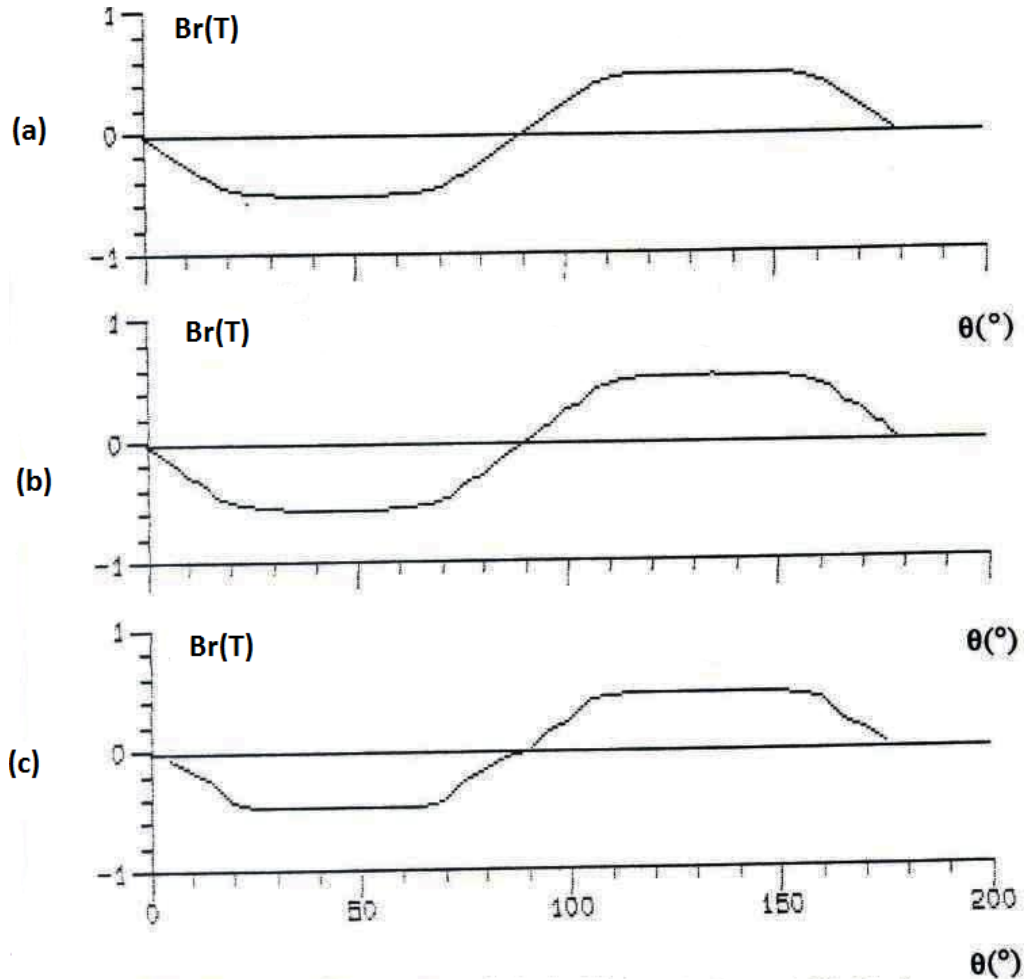
$r_3 = 7.5$ cm in the medium 3

$r_4 = 5$ cm in the medium 4

IV.2 Comparison with other analytical and numerical methods

We have performed a comparative study of a permanent magnet synchronous motor with surfaced magnets carried by the rotor, the stator being assumed slot less. Three methods have been used, the present method, the method of magnetic images with THEBYCHEF polynomials developments and only five images used, and a numerical method based on finite differences. The results show very good agreements (Figs.12a, b, and c). The last method, the pure numeric one presents slight differences, less than 7% with respect to the analytical ones, due to approximations made in that method, and takes three times to be computed with respect to the present method, while the computation time of the method of magnetic is one and half time the one of our method.

The present proposed method which holds the classic advantages of analytical methods e.g the easiest variation of geometric parameters, is then once more well validated by the two other hereby involved methods.



Figs 12.a, b, c: Radial Component owing to three methods of the flux density generated by 60 ° radial and 20 ° azimuth permanent magnets in the air gap. The permeability of the iron parts are supposed finite. Three media are considered.

The Machine Data :

$p = 2$ $R_1 = 7$ cm $R_2 = 5$ cm $R = 6$ cm
 $R' = 5$ cm $\mu_1 = 1000$ $\mu_2 = 1$ $\mu_3 = 1000$
 μ_0 $M = 0.92$ T (NdFeB)

The Studied Points:

$r = 6.5$ cm in the air gap

The present method

The method of magnetic images with five images

A numeric method based on finite differences

V) CONCLUSION

Many cylindrical non saturated machines as well as some electromagnetic devices can be studied by means of semi-analytical methods. In this paper a systematic semi-analytical method has been developed, and allows the calculation of the magnetic potentials and the magnetic flux densities in two-dimensional concentric slot less cylindrical linear media, with different finite magnetic permeability, and a great number of involved magnetic media.

The analytical methods based on the separation of variables, or on the magnetic image methods, are generally used when the number of magnetic media is low (less than three). The method presented in this article, can be applied to great number of magnetic domains within the set hypothesis. This proposed method that has been validated by two other methods, holds many applications, from the designing and modelling of rotating cylindrical electrical machines, to other electromagnetic cylindrical system.

This proposed method is systematic and very easy to use. As it has been verified, the results are obtained more rapidly with a very high accuracy.

VI) ACKNOWLEDGMENTS

Authors would like to present his gratefulness to the University of Ngaoundere in Cameroon and to "Ecole Nationale Supérieure d'Electricité et de Mécanique de Nancy" in France, through its Laboratory "Groupe de Recherches en Electrotechnique et Electronique de Nancy", G.R.E.E.N, for visitor ships and facilities to Andre YOUMSSI.

VII) REFERENCES

- [1] Julien Fontchastagner, Yvan Lefèvre, and Frédéric Messine "Some Co-Axial Magnetic Couplings Designed Using an Analytical Model and an Exact Global Optimization Code" », IEEE Transactions on Magnetics, volume 45, N°03, March 2009

- [2] Seok-Myeong Jang, Hyung-II Park, Jang-Young Choi, Kyoung-Jin Ko, and Sung-Ho Lee “Magnet Pole Shape Design of Permanent Magnet Machine for Minimization of Torque Ripple Based on Electromagnetic Field Theory” », IEEE Transactions on Magnetics, volume 47, N°10, October 2011
- [3] Miroslav Markovic and Yves Perriard “Optimization Design of a Segmented Halbach Permanent-Magnet Motor Using an Analytical Model” », IEEE Transactions on Magnetics, volume 45, N°7, July 2009
- [4] Bernard, N.; Martin, F.; Zaim, M. E.-H. “Design Methodology of a Permanent Magnet Synchronous Machine for a Screwdriver Application” IEEE Transactions on Energy Conversion, volume 27, N°3, 2012
- [5] Pfister, P.-D.; Perriard, Y “Very-High-Speed Slotless Permanent-Magnet Motors: Analytical Modeling, Optimization, Design, and Torque Measurement Methods” IEEE Transactions on Industrial electronics, volume 57, N°1, 2010
- [6] Pierre-Daniel Pfister, and Yves Perriard “Slotless Permanent-Magnet Machines: General Analytical Magnetic Field Calculation” IEEE Transactions on Magnetics, volume 47, N°6, June 2011
- [7] Martin Hafner, David Franck, and Kay Hameyer “Static Electromagnetic Field Computation by Conformal Mapping in Permanent Magnet Synchronous Machines” IEEE Transactions on Magnetics, volume 46, N°8, August 2010
- [8] Damir Ž arko, Drago Ban, and Thomas A. Lipo “Analytical Solution for Electromagnetic Torque in Surface Permanent-Magnet Motors Using Conformal Mapping” IEEE Transactions on Magnetics, volume 45, N°7, July 2009
- [9] K.J.Binns, P.J.Lawrenson, “*Analysis and Computation of Electric and Magnetic Field Problem*” New York: Pergamon Press, pp. 39-59
- [10] A.Youmssi « A Three-Dimensional Semi-Analytical Study of the Magnetic Field Excitation in a Radial Surface Permanent-Magnet Synchronous Motor », IEEE Transactions on Magnetics, volume 42, N°12, December 2006
- [11] Binns, Lawrenson and Trowbridge, “*The analytical and numerical solution of electric And magnetic fields*” London, John Wiley and Sons, 1995
- [12] LJ Wu, ZQ Zhu, D Staton, M Popescu “*Comparison of analytical models for predicting cogging torque in surface-mounted PM machines* ” International Conference on Electrical Machines (ICEM), 2010.
- [13] Wu, L.J.; Zhu, Z.Q.; Staton, D.; Popescu, M.; Hawkins, D “*Analytical prediction of electromagnetic performance of surface-mounted PM machines based on subdomain model accounting for tooth-tips*”, Electric Power Application, 2011.
- [14] Wu, L.J.; Zhu, Z.Q.; Chen, J.T.; Xia, Z.P “*An Analytical Model of Unbalanced Magnetic Force in Fractional-Slot Surface-Mounted Permanent Magnet Machine*”, IEEE Transactions on Magnetic, 2010.
- [15] Z.WU, D.DEPERNET, C.ESPANET ” Conception d’un entraînement électrique à aimants permanents pour une chaîne de traction de véhicule hybride électrique ” European Journal of Electrical Engineering Vol 14/2-3 - 2011 - pp.215-236 - doi:10.3166/ejee.14.215-236
- [16] Yang Shen; Zhu, Z.Q. “*Analytical Prediction of Optimal Split Ratio for Fractional-Slot External Rotor PM Brushless Machines*” IEEE Transactions on Magnetic, 2011.

